ResearchGate

See discussions, stats, and author profiles for this publication at: https://www.researchgate.net/publication/45819538

The Structural Color of Red Rose Petals and Their Duplicates

ARTICLE *in* LANGMUIR · SEPTEMBER 2010

Impact Factor: 4.46 · DOI: 10.1021/la102406u · Source: PubMed

CITATIONS
26

READS
138

6 AUTHORS, INCLUDING:

Mingzhu Li
Chinese Academy of Sciences
51 PUBLICATIONS **709** CITATIONS
SEE PROFILE

Yongmei Zheng
Beihang University (Beijing University of Aer…
74 PUBLICATIONS **2,165** CITATIONS
SEE PROFILE

Weizhi Shen
Chinese Academy of Sciences
16 PUBLICATIONS **209** CITATIONS
SEE PROFILE

Lei Jiang
Yunnan Agricultural University
142 PUBLICATIONS **5,002** CITATIONS
SEE PROFILE

Available from: Yongmei Zheng
Retrieved on: 31 January 2016

Langmuir
Article
pubs.acs.org/Langmuir
© 2010 American Chemical Society

The Structural Color of Red Rose Petals and Their Duplicates

Lin Feng,*,† Yanan Zhang,§ Mingzhu Li,‡ Yongmei Zheng,‡ Weizhi Shen,‡ and Lei Jiang‡

†*Department of Chemistry, Tsinghua University, Beijing 100084, P. R. China,* ‡*Institute of Chemistry, Chinese Academy of Sciences, Beijing 100080, P. R. China, and* §*College of Chemistry, Jilin University, Changchun 130023, P. R. China*

Received June 14, 2010. Revised Manuscript Received August 7, 2010

The observation of the surface of a red rose petal indicates that there are micropapillae on the surface and many nanofolders exist on each papilla. Here, much tinier nanorods with periodic pattern on the nanofolders can be seen by in situ atomic force microscopy (AFM). Angle-resolved UV−vis spectral measurement and reflectance UV−vis spectra by immersion red rose petal in solvents with different refractive indices demonstrate that such periodic nanostructures can induce structural color. The combination of structural color, driven by the nanostructures, and chemical color, driven by pigments, provide flowers bright color and special functions for human and animals' visual system. Biomimic polymer films, that fabricated by duplicating the petal's hierarchical micro/nano structures, exhibit only structural color by UV−vis spectra since there is no pigment introduced.

Introduction

Flowers attract people for their beautiful appearance and brilliant colors. For many years, people paid much attention to enjoy diverse flowers but rarely notice why they are so fascinating and can long-lived in various environments such as suffering acid rain and exposure on hot sun. On the other hand, because the flowers are visually dull to insect owing to the weak reflection of light across the whole range of the insect visual spectrum, it is confused how the flowers attract insect for pollination. Traditionally, people believe that the color of the flowers is caused by pigments, so-called chemical color. Plant pigments have been thoroughly studied from a biochemical perspective, and their synthesis and regulation have been characterized by molecular genetics. However, colors will appear dull or muted resulting from only chemical color since pigments are not very good at absorbing all but a very few wavelengths.[1]

Color production in nature takes advantage of either chemical or structural color. Structural color originate from patterned microstructures has been proved to provide some insects and birds charming colors, e.g., some tropical butterflies, peacock feathers and some beetles.[2−8] The dazzling iridescence seen in these species arises from natural optical phenomena, the brightest of which originate in nanoscale structures that produce ultrahigh reflectivity and narrow-band spectral purity. Since the introduction of the photonic band gap concept, the creation of materials exhibiting a periodic modulation of the dielectric constant has attracted much interest.[9,10] Such materials, known as photonic crystals or opal, diffract photons from a lattice of dielectric planes in a manner analogous to the behavior of electrons with respect to an atomic crystal lattice. Although structural color has been well characterized in animals, very little has been studied in plants. Glover et al. revealed the floral iridescence in *Hibiscus trionum* and *Tulipa* species, produced by diffractive optics, which is identified to be important in pollinator attraction.[1,11] This study opened a new look on structured color in flowers and its function.

We reported recently the petal effect: there is a close array of micropapillae on the surface of the petal of red rose (*rosea Rehd*), and many nanofolders exist on each papilla top.[12] These hierarchical micro- and nanostructures provide superhydrophobicity with water contact angle higher than 150° and a high adhesive force with water. This character imparts flowers special properties in that small water droplets can stay stably on the petals maintaining their fresh look, while the bigger ones, such as raindrops, can roll off. Here, we disclose the other important aspect of structural color for the red rose petals. The observation of the surface of a red rose petal by in situ AFM indicates that there are much tinier nanorods periodically patterned on the nanofolders of a red rose petal. Angle-resolved UV−vis spectral measurement and reflectance UV−vis spectra by immersion red rose petal in solvents with different refractive indices demonstrate that such nanostructures can induce structural color. A mixing of chemical and structural colors on red rose petal provides the flowers' bright appearance, durability, and the animal pollination. Biomimetic polymer films, which were fabricated by duplicating the petal's microstructures, exhibit only structural color by UV−vis spectra since there is no pigment introduced into these films. The straightforward proof that the nanostructures are contributing to the structural color of a red rose could be of great help in understanding structural color in flowers and give useful information for the design of biomimetic optical devices.

Experimental Section

Commercial red rose petals were cut into small pieces 1 cm × 2 cm in size and used directly for AFM and angle-resolved UV−vis measurement after flushing off the dirt on the surface with water.

*Corresponding author. E-mail: fl@mail.tsinghua.edu.cn.

(1) Glover, B. J.; Whitney, H. M. *Ann. Bot.* **2010**, *105*, 505.
(2) Vukusic, P.; Sambles, J. R. *Nature* **2003**, *424*, 852.
(3) Vukusic, P.; Sambles, J. R.; Lawrence, C. R.; Wootton, R. J. *Nature* **2001**, *410*, 36.
(4) Vukusic, P.; Sambles, J. R.; Lawrence, C. R. *Nature* **2000**, *404*, 457.
(5) Zi, J.; Yu, X.; Li, Y.; Hu, X.; Xu, C.; Wang, X.; Liu, X.; Fu, R. *Proc. Natl. Acad. Sci. U.S.A.* **2003**, *100*, 12576.
(6) Parker, A.; Welch, V. L.; Driver, D.; Martini, N. *Nature* **2003**, *426*, 786.
(7) Parker, A.; McPhedran, R. C.; McKenzie, D. R.; Botten, L. C.; Nicorovici, N. A. P. *Nature* **2001**, *409*, 36.
(8) Kinoshita, S.; Yoshioka, S. *ChemPhysChem* **2005**, *6*, 1442.
(9) Yablonovitch, E. *Phys. Rev. Lett.* **1987**, *58*, 2059.
(10) John, S. *Phys. Rev. Lett.* **1987**, *58*, 2486.
(11) Whitney, H. M.; Kolle, M.; Andrew, P.; Chittka, L.; Steiner, U.; Glover, B. J. *Science* **2009**, *323*, 130.
(12) Feng, L.; Zhang, Y.; Xi, J.; Zhu, Y.; Wang, N.; Xia, F.; Jiang, L. *Langmuir* **2008**, *24*, 4114.

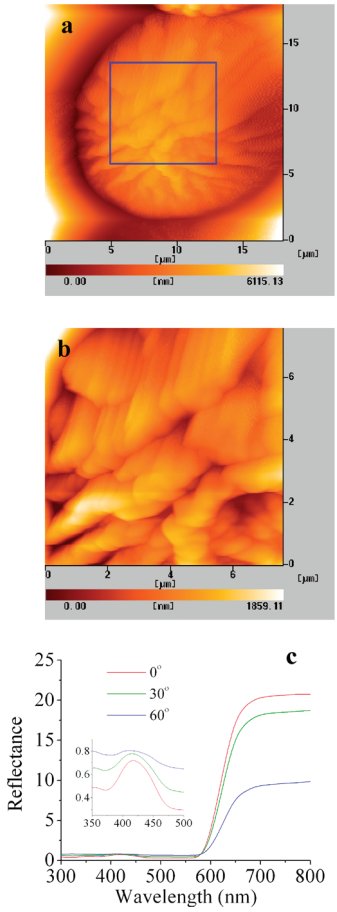

Figure 1. (a) AFM images of a red rose petal's surface, showing the hierarchical micropapillae and nanofolders structure. (b) Enlarged image of the square area in a, showing the nanorods periodically patterned on the nanofolders. (c) UV−vis reflectance spectra of a red rose petal at different incident angles, showing two peaks of both pigment and structural colors. The inset shows an enlarged plot of the region between 350 and 500 nm to illustrate the change in stop-band.

The small pieces of petal were clipped by two slide glasses to form a sandwich structure, and then put into vacuum oven to remove the water. These dried petals were immersed into different solvents for 48 h until they were completely filled with the solvents for UV−vis measurement.

The small pieces of petal were immersed into DMF for 24 h to remove the pigment, dried and immersed into different solvent for UV−vis measurement.

Poly(vinyl alcohol) (PVA) and polystyrene (PS) films were fabricated using the method described in ref 12.

The morphological characterization of the red rose surfaces was examined by using AFM (SII Seiko Instruments Inc., SPI 3800N in the tapping mode), while the morphology of the polymer films were observed by scanning electronic microscope (SEM, JEOL, JSM-6700F at 3 kV). UV−vis spectra were acquired by Hitachi UV-4100 spectrophotometer.

Results and Discussion

Parts a and b of Figure 1 show the AFM images of a fresh red rose petal measured in ambient atmosphere. Micropapilla with the diameter about 16 μm and nanofolders with the width about 730 nm can be found under low resolution (Figure 1a), which is in correspondence to that of the SEM image.[12] The enlarged image (Figure 1b) indicates that there are periodic nanorods patterned on each nanofolder. The average diameter of the rods is about 200 nm and the period (the center-to-center distance of the rods) is about 240 nm. The periodic nanorods array observed here suggest that the red rose petal surfaces actually own the photonic crystal structure. In this case, structural color may be produced similar to that on butterflies, beetles, and peacock feathers. Figure 1c shows the measured reflectance by using angle-resolved UV−vis spectral instrument. The UV−vis spectra of the red rose surface show two peaks: the peak around 684 nm, assigned to the pigment, is invariable with the variety of incident angle. The other peak appears is considered to originate from the diffraction of the 1D ordered structure of nanorods shown in Figure 1b, so-called optical stop bands, which shifts toward the blue wavelength as well as the peak height decrease with increasing angle. When the incident angle changed from 0° to 60°, a shift of approximate 8 nm occurs from 417 to 409 nm (insert in Figure 1c). These results indicate that there're both chemical color and structural color on red rose petal. The chemical color is determined by pigments on the cells,[13] while the structural color comes from the nanosized structures. The combination of the two colors provides red rose bright color and can reflect wavelengths of light perceptible for both humans and pollinating animals.

SEM images indicate that the micro and nano structures can well maintain except for the shrink after the red rose petal are dried (see Supporting Information, Figure S1). Therefore, to further confirm the structural color in a red rose, we put the fresh petals (1 cm × 2 cm) into the vacuum drying oven to remove water, and then immersed them into different solvents to fill the air holes between microstructured papillae, nanostructured folders, and nanostructured rods. UV−vis spectra indicate that the shift in the position of the stop bands to higher wavelengths upon filling of the void spaces of micro/nanostructured materials with solvents is greater for larger values of the solvent refractive index. The suitability of the red rose as a refractive index sensor was investigated by immersing in solvents with different refractive indices: methanol (n = 1.329), water (n = 1.340), ethanol (n = 1.360), THF (n = 1.407), DMF (n = 1.431), and chloroform (n = 1.446).[14] It has also been proved that red rose petals have the strong antierosion properties, i.e., the micro/nanostructures can maintain well after they were immersed in the above-mentioned organic solvents, as well as in acidic, basic, or salt solution (see Supporting Information, Figure S2). The UV−vis reflectance spectra of the red rose in these solvents are shown in Figure 2a. Both the pigment and the structure peaks depend on the solvents. The stop-band peak shifts by 13 nm from 443 nm (in methanol) to 456 nm (in chloroform) when the refractive index increases from 1.329 to 1.446. The pigment peak also shifts by 31 nm from 695 to 726 nm due to the difference of the solvent polarity.

To eliminate the pigment color, we further immersed the fresh red rose petals into DMF for 24 h, after which the petals appeared to have a white color as observed with a naked eye and the solvent appeared to have a red color. The "white petal" was again immersed into solvents with different refractive indices. From the UV−vis spectra (Figure 2b), we can clearly seen that only one structural color peak can be seen at about 411−424 nm after immersion into methanol, DMF, water and ethanol; however, there are still two peaks after immersion into chloroform, THF, and hexane (n = 1.375). The reason is that the red pigment color can be recovered at the edge of the petal in the latter solvents. The UV peaks obviously shift to higher wavelengths upon filling the solvents with larger values of refractive index in both situations.

(13) Ozawa, A.; Uehara, T.; Sekiguchi, F.; Imai, H. *Opt. Rev.* **2009**, *16*, 458.
(14) Gu, Z.; Horie, R.; Kubo, S.; Yamada, Y.; Fujishima, A.; Sato, O. *Angew. Chem., Int. Ed.* **2002**, *41*, 1154.

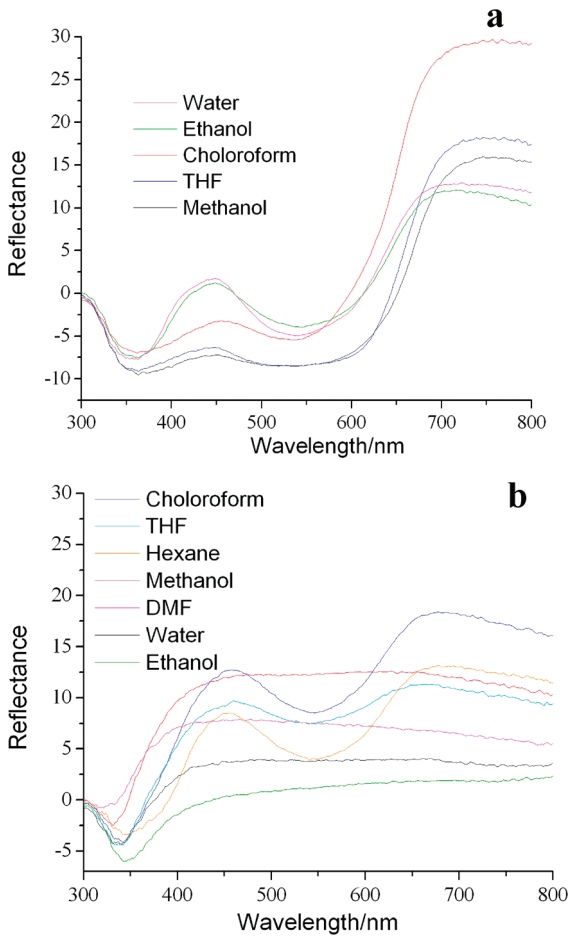

Figure 2. UV−vis reflectance spectra in different media (methanol (n = 1.329), water (n = 1.340), ethanol (n = 1.360), hexane (n = 1.375), THF (n = 1.407), DMF (n = 1.431) and chloroform (n = 1.446)) of (a) a dried red rose petal or (b) a red rose petal after removal of the pigment by being immersed into DMF.

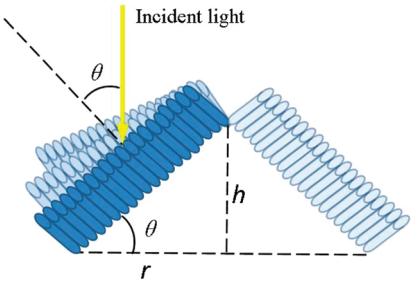

Figure 3. Schematic model of one micropapilla on the surface of a red rose petal, showing the multiple structures: nanofolders composed of papilla, and nanorods with periodic array patterned on each nanofolder.

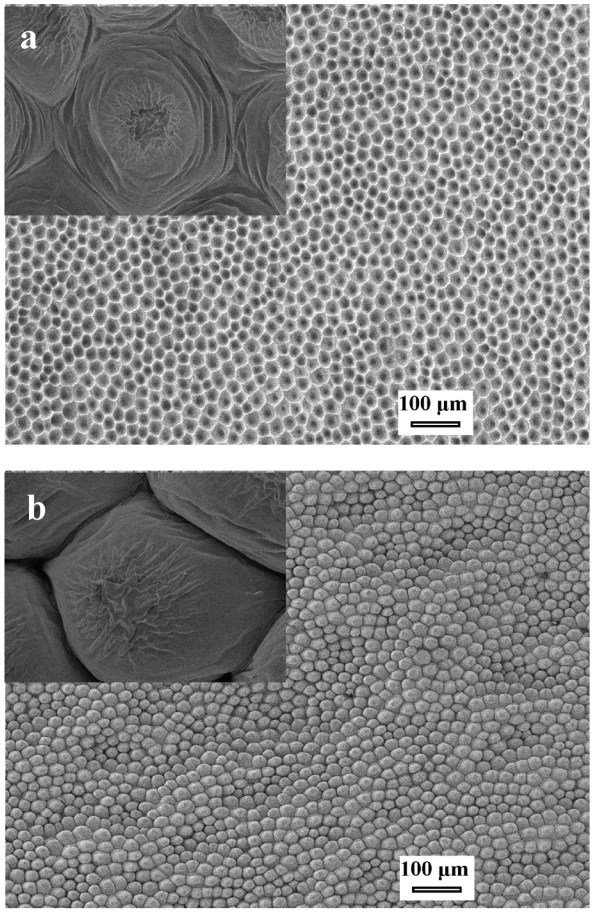

Figure 4. SEM images of the duplicated (a) PVA film with inverse petal structure and (b) PS film with similar petal structure (insert are the enlarged image of one papilla). (c) UV−vis reflectance spectra of the prepared PVA film and PS film, both showing a stop band peak that produce structural color.

Moreover, the peaks for structural color shift to about 451−457 nm and that for the pigment shift to about 662−671 nm. These changes are due to the mutual effect of structural color and chemical color.[11]

The relationship between the nanostructures and the optical stop bands can be theoretically calculated by the optical Bragg law, $\lambda = 2dn_{\mathrm{eff}}$, where n_{eff} is the effective refractive index of the system, and d is the period. For the fresh red rose petal, n_{eff} is 1.340 considering the void spaces are filled with water. d can be calculated as D sin θ, where D is 240 nm measured from Figure 1b and θ is the angle between the direction of incident light and the nanorods array. Figure 3 illustrates the model of the multiple structures on the surface of the red rose petal, according to which sin θ is $h/(h^2 + r^2)^{1/2}$, where h is the height of the micropapilla and r is the radius of the micropapilla. On the basis of the SEM image we reported before, h is 7 μm and $2r$ is 16 μm;[12] thus, λ can be calculated as 423 nm. This result is consistent with the experimental data in Figure 1c within the measurement and calculation error. On the other hand, it can be easily found from the optical Bragg law that increasing n_{eff} will result in the shift of the optical stop band to higher wavelength, which is also

accordant with the result of the solvent-dependent system shown in Figure 2.

It has been proved to be a good strategy to fabricate biomimetic polymer films by using the red rose petal as a duplicated template and the solvent-evaporation-driven nanoimprint pattern transfer process at room temperature. This convenient method has the merit of using the natural petals, an environment friendly material, as the template, which is not accessible in many other conventional techniques.[15−17] Therefore, diverse surface structures of natural leaves and petals became inspiring media for the development of biomimetic surfaces. The as-obtained duplicated poly(vinyl alcohol) (PVA) film with inverse petal structures and polystyrene (PS) film with the similar petal's surface structure are both superhydrophobic with high adhesive force to water.[12] It is interesting that after the introduction of the red rose petal's hierarchical structure into the PVA and PS films, they also have structural color. Parts a and b of Figure 4 show the SEM images of the duplicated PVA film and PS film. The PVA film is characterized as an inverse petal's structures since it is duplicated from the rose petal, while the PS film has a similar petal's structure that is duplicated from the textured PVA film. It is worth to note that the two polymer films have both micro and nanostructures shown in the large scale images and the individual insert images, that is, the hierarchical structures can be successfully and accurately duplicated from rose petal. According to the analysis of the rose petal that the periodic nanostructures can give rise to structural color, we expect that the duplicated polymer films also have the same effect. UV−vis spectra of PVA and PS films are given in Figure 4c, showing the stop band peak appear at 405 and 416 nm respectively, which are consistent with that of the red rose petal. However, there is no peak appearing around 600−700 nm since there is no pigment introduced into the polymer films. As a result, we have designed a material by mimicking the microstructure of petal's surfaces that incorporates both the superhydrophobicity and structural color. The hierarchical micropapillae and nanofolders are contributed to superhydrophobicity, while the periodic nanorods are responsible to the structural color. This study should be of great biological and technological importance. In recent years, several strategies have been used for the creation of photonic crystals with a periodic array,[18−32] including the chemical methods of colloidal self-assembly and colloidal crystal templating, the microfabrication techniques of mechanically drilling holes within a dielectric slab or stacking logs of a dielectric material, and holographic patterning using multiple laser beams. Other interesting surface properties such as superhydrophobicity are also expected on the photonic crystal but have rarely been observed. Materials exhibiting both superhydrophobicity and structural colors could provide a number of unique technological applications, including optical devices.

Conclusions

In conclusion, nature offers an extremely diverse pool of biological master surfaces with structure-dependent surfaces properties. On the basis of the periodic surface nanostructures characterized by AFM, red rose petals have shown the special optical property of structural color. Duplicated polymer films with structural color have been generated by using red rose petals as templates and a simple duplicate technique. The technique allows the duplication of complex surface micro and nano structures in a fast and cost-efficient way. The transfer of complex architectures with unique optical property from red rose petals onto technical surfaces implies a great potential for the development of new biomimetic surfaces.

Acknowledgment. The authors thank the project funded by the National Natural Science Foundation of China under Grant No. 50703020 and the National Key Basic Research and Development Program of China under Grant No. 2009CB930602.

Supporting Information Available: Figures showing the microstructures of the surface of the dried red rose petal after it was immersed in acidic, basic, or salt solution, as well as in organic solvents. This material is available free of charge via the Internet at http://pubs.acs.org.

(15) Schulte, A. J.; Koch, K.; Spaeth, M.; Barthlott, W. *Acta Biomater*. **2009**, *5*, 1848.
(16) Schweikart, A.; Zimin, D.; Handge, U. A.; Bennemann, M.; Altstädt, V.; Fery, A.; Koch, K. *Macromol. Chem. Phys*. **2010**, *211*, 259.
(17) Lee, S. M.; Kwon, T. H. *Nanotechnology* **2006**, *17*, 3189.
(18) Shkunov, M. N.; Vardeny, Z. V.; DeLong, M. C.; Polson, R. C.; Zakhidov, A. A.; Baughman, R. H. *Adv. Funct. Mater*. **2002**, *12*, 21.
(19) Campbell, M.; Sharp, D. N.; Harrison, M. T.; Denning, R. G.; Turberfield, A. J. *Nature* **2000**, *404*, 53.
(20) Yu, A.; Meiser, F.; Cassagneau, T.; Caruso, F. *Nano Lett*. **2004**, *4*, 177.
(21) Vlasov, Y. A.; Bo, X.; Sturm, J. C.; Norris, D. J. *Nature* **2001**, *414*, 289.
(22) Blanco, A.; Chomski, E.; Grabtchak, S.; Ibisate, M.; John, S.; Leonard, S. W.; Lopez, C.; Meseguer, F.; Miguez, H.; Mondia, J. P.; Ozin, G. A.; Toader, O.; Driel, H. M. *Nature* **2000**, *405*, 437.
(23) Braun, P. V.; Wiltzius, P. *Nature* **1999**, *402*, 603.
(24) Saunders, A. E.; Shah, P. S.; Sigman, M. B.; Hanrath, T.; Hwang, H. S.; Lim, K. T.; Johnston, K. P.; Korgel, B. A. *Nano Lett*. **2004**, *4*, 1943.
(25) Kubo, S.; Gu, Z.; Takahashi, K.; Fujishima, A.; Segawa, H.; Sato, O. *Chem. Mater*. **2005**, *17*, 2298.
(26) Rugge, A.; Park, J. S.; Gordon, R. G.; Tolbert, S. H. *J. Phys. Chem. B* **2005**, *109*, 3764.
(27) Zhou, Z.; Zhao, X. *Langmuir* **2005**, *21*, 4717.
(28) Kubo, S.; Gu, Z.; Takahashi, K.; Fujishima, A.; Segawa, H.; Sato, O. *J. Am. Chem. Soc*. **2004**, *126*, 8314.
(29) Viel, B.; Ruhl, T.; Hellmann, G. P. *Chem. Mater*. **2007**, *19*, 5673.
(30) Orilall, M. C.; Abrams, N. M.; Lee, J.; DiSalvo, F. J.; Wiesner, U. *J. Am. Chem. Soc*. **2008**, *130*, 8882.
(31) Bohaty, A. K.; Zharov, I. *Langmuir* **2006**, *22*, 5533.
(32) Honda, M.; Kataoka, K.; Seki, T.; Takeoka, Y. *Langmuir* **2009**, *25*, 8349.